

Decolorization of Cationic Dye from Aqueous Solution by Multiwalled Carbon Nanotubes

Salwa H. Ahmed^{1*}, Ekehwanh A. Rasheed², Luma A. Rasheed³, Firas R. Abdulrahim⁴

¹ Department of Environmental Engineering, College of Engineering, Tikrit University, Iraq

² Department of Chemical Engineering, College of Engineering, Tikrit University, Iraq

³ Department of Electrical Engineering, College of Engineering, Tikrit University, Iraq

⁴ Ministry of Oil, Iraq Drilling Company, HSE Department, Kirkuk, Iraq

* Corresponding author's e-mail: dr.salwahadi@tu.edu.iq

ABSTRACT

Methylene blue is a synthetic and cationic dye that finds utility in different fields including pharmaceutical, paper, textile, printing, carpet, and photography industries. Adsorption is a very effective technique to decolorize contaminated wastewater. This study aimed to determine the efficacy of Multiwalled Carbon Nanotubes (MWCNTs) as an adsorbent for decolorization of MB dye from aqueous solutions. The study examined various characteristics affecting adsorption, including concentration of dye, pH value, dosage of MWCNTs, and contact time. The results that growing the adsorbent dosage from (25 to 120) mg increased the dye efficiency rate from 62% to 98%, respectively, were shown. The study also evaluated pH, which is among the most critical factors influencing removal efficiency. The best pH for the removal efficiency was 6 at an initial concentration of MB dye 20 mgL⁻¹, a contact time 60 min, and an MWCNT dosage 100 mg. Langmuir, Freundlich, and Temkin isotherms were used to describe the adsorption equilibrium. The Langmuir isotherm with an R² value of 0.9968 and a maximum capacity for adsorption of 19.6 mgg⁻¹ provided a suitable fit for the data of the experiment. In comparison between the suitability of kinetic models pseudo-first-order, pseudo-second order, and Weber–Morris, the kinetics model's correlation value was shown to be greater than that of the pseudo-second order kinetic model with an R² value of 0.9982.

Keywords: multiwalled carbon nanotubes, methylene blue, adsorption, adsorption equilibrium, the kinetics model.

INTRODUCTION

The presence of dangerous dyes in the stream of water is currently one of the most important main environmental issues (Robati et al. 2016). The number of commercially available dyes exceeds 100,000 dyes, and over 700,000 tons of dyestuff are produced every year. Dyes will be categorized based on their structure as cationic and anionic (Mahvi et al. 2012, Almhana et al. 2022). Dyes are classified as organic compounds that are aromatic and ionic (Sanghavi et al. 2015).

Industries rely heavily on dyes to produce foodstuffs, leather, paper, cosmetics, textiles, and many other products. However, many of these dyes are not easily biodegradable and can have carcinogenic or toxic effects on humans and

animals. Methylene Blue Dye (MB) is a toxic colorant that can cause mutation, cancer, and skin problems upon contact (Ghosh et al. 2022a). Hence, colorization from industrial wastewater is an essential area of applied and basic research (Altıntig et al. 2017).

Numerous technologies have been developed to address the wastewater contaminated with organic contaminants, including electrochemical methods, precipitation, and coagulation-flocculation (Ibrahim, 2021) membrane filtering (Ahmed et al. 2021), advanced oxidation (Ghosh et al. 2022b; Mohammed et al. 2021), ion exchange, photocatalytic degradation (Almhana et al. 2022), and adsorptive removal (Robati et al. 2016; Badran and Khalaf, 2020). Because of its high efficiency, cleanliness, resistance to harmful toxins, and ease

of operation, adsorption has become one of the most favored methods for treating wastewater (Badran and Khalaf, 2020). Activated carbon (Li et al. 2013), graphene nanosheets (Machado et al. 2011), multiwalled carbon nanotubes (Fan et al. 2013), rice sawdust, crushed brick (Robati et al. 2016), rice husk (Georgiou et al. 2007; Saleh and Gupta, 2012), magnetic chitosan/ graphene oxide composite (Onal, 2006) waste tires rubber ash (Ahmed, 2017), and several other low-cost adsorbents (Mohammed et al. 2014; Robati et al. 2016; Mohsen et al. 2023) have been used in the previous studies to effectively and quickly eliminate as well as adsorb harmful dyes (Robati et al. 2016).

In Figure 1, Multiwalled carbon nanotubes (MWCNTs) have a very high surface area, which means they can absorb many molecules.

This is because they consist of a long, thin tube with a hollow core. The surface area of MWCNTs must be up to 1000 times larger than that of activated carbon. These MWCNTs have several distinguishing characteristics, including high porosity, chemical inertness, chemical stability, a carbon-constructed surface, and nanometer-sized channels (Sanghavi et al. 2015). They are thermally and electrically conductive. MWCNTs are stronger than most known materials in both theoretical computations and tests. Furthermore, the mass of MWCNTs is much lower than that of the most used robust materials, such as steel and aluminum. These properties make MWCNTs a favorable material for different uses, including sorbents, electronics, composite materials, energy storage, and biomedical applications.

MWCNTs have been shown to have a high capacity for removing a wide range of contaminants, including resorcinol, aniline, ethyl benzene, and phenol (Robati et al. 2016; Sanghavi et al. 2015). Iraq discharges a considerable amount of dye-contaminated wastewater from the textile industry into the Tigris River, making it necessary to find a quick and effective technology that can directly extract these dyes from wastewater before discharging it into the river (Sanghavi et al. 2015; Muhaisen et al. 2021). This study utilized MWCNTs as an adsorption material to eliminate MB dye from aqueous solutions under reference conditions, including pH solution, initial MB dye concentration, MWCNTs dosage, and contact time as well as to investigate the isotherm and kinetics of MB adsorption from aqueous solutions using MWCNTs.

EXPERIMENTAL WORK

Adsorbent material

MWCNTs were used as a commercial adsorbent and sold from Nanotech Port Co. in Shenzhen, China. MWCNTs have been extensively examined for their potential as adsorbent material because of their high surface area, unique structure, as well as mechanical and chemical stability.

Dye

The dye for this research was purchased from commercial markets, Iraq. MB is a basic dye and has a deep blue color in its oxidized form and fragrant heterocyclic essential color with a molecular weight of dye $319.85 \text{ g mol}^{-1}$ (Sahu et al. 2020). The chemical formula of the Methylene Blue dye is $\text{C}_{16}\text{H}_{18}\text{N}_3\text{ClS}$. It is very soluble in water and ethanol. Methylene blue is relatively stable under normal conditions, but it can be degraded by light and heat. It is low in toxicity, but it can be harmful if ingested or inhaled in large quantities (Sabar et al. 2020).

Adsorption experiment

The work batch experiments were conducted in the laboratory of the Department of Environmental Engineering in the College of Engineering and the central laboratory at Tikrit University. The absorbencies of methylene blue dye were

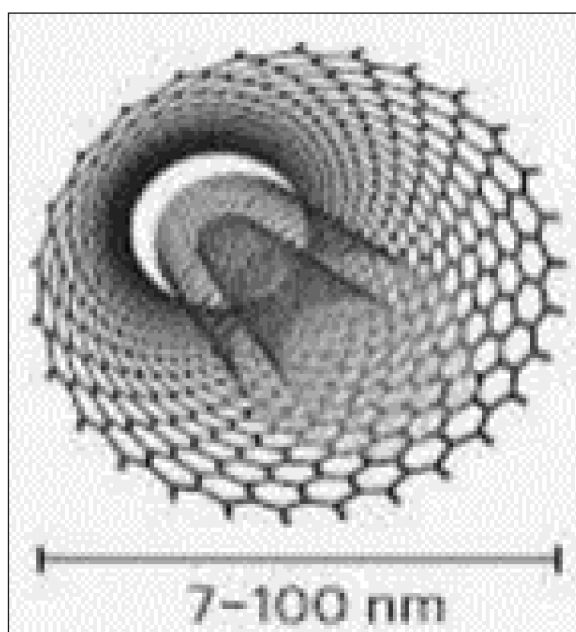


Figure 1. Photo of MWCNTs

determined using a JASCO UV-VIS/530 spectrophotometer at a λ_{\max} of 663 nm, following standard methods. During the study, 1000 mg of MB dye powder was dissolved in one liter of deionized water to create the stock solution and further diluted to initial concentrations ranging from 20 to 120 mgL^{-1} . MWCNTs adsorbent at the dosage of 25 to 120 mg were added to 100 ml of dye solutions with a concentration of dye 100 mgL^{-1} in 250 ml conical flasks, which were shaken at 200 rpm and $25 \pm 2^\circ\text{C}$ for predefined time intervals (every 10 minutes), and the MB dye concentrations were measured using a UV-spectrophotometer after sorption. The effects of deferent factors such as pH were evaluated by adjusting the pH of the solutions with HCl of 0.1M or NaOH of 0.1M, and the pH value was measured using a pH instrument (Hanna 211, Romania). Capacity of adsorption (q) in mgg^{-1} was determined using the Eq. 1:

$$q = \frac{C_0 - C_f}{m} V \quad (1)$$

where: C_0 and C_f – the initial and final concentrations of dye solution in mgL^{-1} , m – the mass of MWCNTs adsorbent in g, V – the volume of dye solution in L. Removal effectiveness (R%) of each dye was calculated using the Eq. 2:

$$R\% = \frac{C_0 - C_f}{C_0} \times 100 \quad (2)$$

EQUILIBRIUM ISOTHERM MODELS

To identify the homogeneous and heterogeneous properties of the adsorbent, the experimental data were analyzed using the Langmuir, Freundlich, and Temkin models. The equilibrium isotherms were investigated to describe the adsorption process, and the best fit was determined according to the correlation coefficients (R^2) closest to 1. High R^2 values indicate the relevance of the experimental data to the model isotherm or kinetics. The linear equations for equilibrium isotherms are as follows (Langmuir equation):

$$q_e = \frac{q_m K_c C_e}{1 + K_c C_e} \quad (3)$$

where: q_e , (mgg^{-1}) – the dye quantity adsorbed per gram of the adsorbent at equilibrium conditions; C_e , (mgL^{-1}) – the adsorbate concentration at equilibrium; q_m , (mgg^{-1}) – maximum single layer coverage

ability; K_c , (Lmg^{-1}) – constant of Langmuir isotherm.

In the beginning, the equilibrium of gas molecules on a metal surface was determined utilizing the Langmuir isotherm. The straight type of the Langmuir condition is communicated as Eq. 4 (Mahvi et al. 2012):

$$\frac{C_e}{q_e} = \frac{1}{K_c q_m} + \frac{C_e}{q_m} \quad (4)$$

Freundlich equation:

$$q_e = K_f C_e^{1/n} \quad (5)$$

where: q_e (mgg^{-1}) – the dye absorbed quantity per gram of the adsorbent at equilibrium; K_f (mgg^{-1}) – constant of Freundlich isotherm; n , intensity of adsorption; C_e (mgL^{-1}) – the adsorbate equilibrium concentration. The constant K_f is a convergent index of the capability of adsorption, and $1/n$ is a function of the adsorption strength in the process of adsorption.

In 1906, Freundlich introduced an empirical isotherm model that is now commonly known as the Freundlich isotherm. This model can explain non-ideal sorption on heterogeneous surfaces and multilayer sorption. The linearized form of the Freundlich equation, Eq. (6), is given below.

$$\log q_e = \log K_f + \frac{1}{n} \log C_e \quad (6)$$

Temkin equation:

$$q_e = B_1 \ln (K_t C_e) \quad (7)$$

The adsorptive adsorbent interactions are explicitly considered by a factor in the Temkin isotherm. Linearizing the Temkin equation, Eq. (8), gives (Moussavi and Khosravi, 2010).

$$q_e = B_1 \ln K_t + B_1 \ln C_e \quad (8)$$

where: q_e – adsorbed quantity at equilibrium in mgg^{-1} , C_e – adsorbate concentration in solution at equilibrium mgL^{-1} , B_1 – a constant associated to the heat of adsorption, known as $B = RT/b$ (dimensionless), R – constant of gas ($8.314 \text{ Jmol}^{-1} \text{ K}^{-1}$), T – absolute temperature in K, b – Temkin Constant in Jmol^{-1} , K_t – Temkin Constant isotherm in Lg^{-1} .

ADSORPTION KINETIC MODELS

The adsorption kinetics were examined to determine the capacity of the dye for mass transfer to MWCNT sites (Hong et al. 2009). When analyzing isotherm data, it is necessary to create an equation that closely constitutes the results and can be applied for design reasons (Baccar et al. 2009). In this research, pseudo-first order, pseudo-second order, and Weber-Morris kinetic models for 20 mgL⁻¹ of dye were investigated, also referred to as intra-particle diffusion (Ahmed et al. 2023). The following equations describe the kinetic models and their applications:

Equation of pseudo-first order:

$$\frac{dq_t}{dt} = k_1(q_e - q_t) \quad (9)$$

Pseudo-first order equation in the form of the linearized:

$$\log(q_e - q_t) = \log(q_e) - \frac{1}{2.303} k_1 t \quad (10)$$

where: q_e (mgg⁻¹) – the quantity adsorbed at equilibrium, q_t (mgg⁻¹) – the quantity adsorbed at time t , k_1 (min⁻¹) – the rate constant for the pseudo-first-order sorption.

Equation of pseudo-second order:

$$\frac{dq_t}{dt} = k_2(q_e - q_t)^2 \quad (11)$$

The following is the form of the linearized pseudo-second order equation:

$$\frac{t}{q_t} = \frac{1}{h} + \frac{1}{q_e} t \quad (12)$$

where: k_2 (gmg⁻¹ min⁻¹) – the rate constant of the pseudo-second-order kinetic equation, q_e (mgg⁻¹) – the maximum sorption capacity in, q_t (mgg⁻¹) – the amount of sorption at time t , $h = k_2 q_e^2$.

Equation of Weber-Morris.

$$q_t = k_{id}(t)^{0.5} + C \quad (13)$$

The following is the form of the linearized Weber-Morris Equation (Weber and Chakkra-vorti, 1974):

$$\log q_t = \log k_{diff} + 0.5 \log(t) \quad (14)$$

where: q_t , mgg⁻¹, the amount of dye adsorbed at time t ; K_{diff} , mg g⁻¹ min^{-1/2}, the rate constant for intra-particle diffusion.

RESULTS AND DISCUSSION

Characteristics of MWCNTs

Fig. 2 show the X-ray diffraction analysis of the raw MWCNTs and reveals prominent peaks at 2θ approximately 25.91 and 73.26 degrees, corresponding to the (002) and (100) reflections of graphite, respectively, and are consistent with the Joint Committee of Powder Diffraction Studies (JCPDS) reference number 96-101-1061. These findings align with previous studies conducted by (Chen et al. 2009; Gupta et al. 2011; Oh et al. 2010). The sharpness of the C (002) peak signifies the graphite-like structure of the MWCNTs and is a crucial indicator for determining their crystal size and interlayer spacing (Jurkiewicz et al. 2018). The untreated MWCNTs used in the analysis have an outer diameter smaller than 10 nm, contain less than 5% amorphous carbon, and have lengths ranging from 5 to 15 μ m. To eliminate the amorphous carbon content, the MWCNTs underwent thermal treatment at 400°C for 60 minutes, resulting in a weight loss of less than 1%. The XRD characteristics of the analyzed MWCNTs indicate a significant surface area, which facilitates effective adsorption of dyes like methylene blue, as demonstrated in a study by Abdel-Ghani et al. 2015.

To investigate the potential alterations in the surface morphology resulting from the synthesis of the adsorbent or the adsorption process, scanning electron microscopy (SEM) was employed using the TESCAN-Vega3 SEM device from the Czech Republic. Fig. 3 explains the cases of the SEM images of the Multiwalled Carbon Nanotubes (MWCNTs) in the form of dispersed nanocomposites and active particles. It is worth noting that the adsorbents employed in this study were previously synthesized and characterized, as mentioned in reference (Robati et al. 2016).

The FTIR spectra of MWCNTs shown in Fig. 4. A Shimadzu FTIR spectroscopy instrument from Japan was used to analyze Multiwalled Carbon Nanotubes (MWCNTs) and defined the functional category present and significance in the removal process. The analysis covered 500–4000 cm⁻¹ wave number range, which includes well-known adsorbent groups. The provided FTIR spectrum exhibits specific peaks at distinct wavenumbers, which can indicate various functional category or chemical bonds. The summary of the possible interpretations is as follows: the presence of alcohols or phenols is suggested by

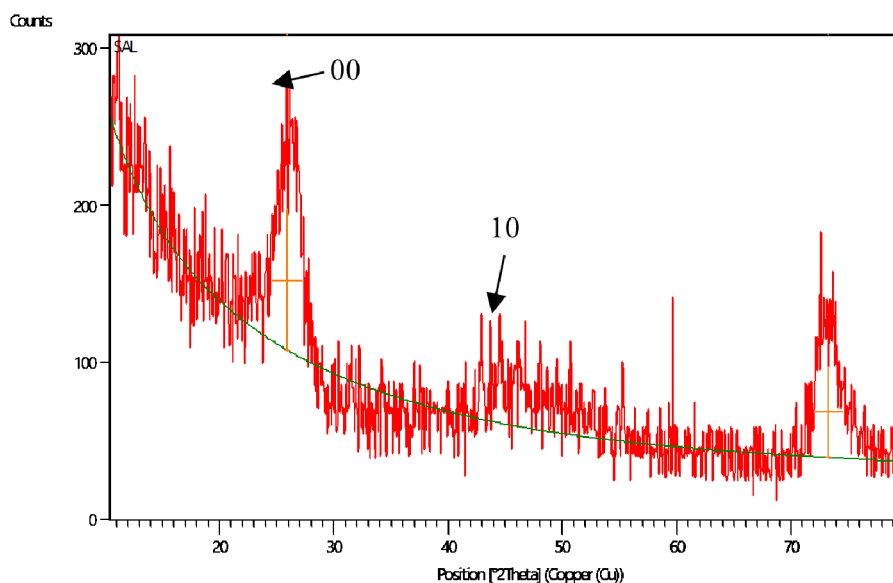
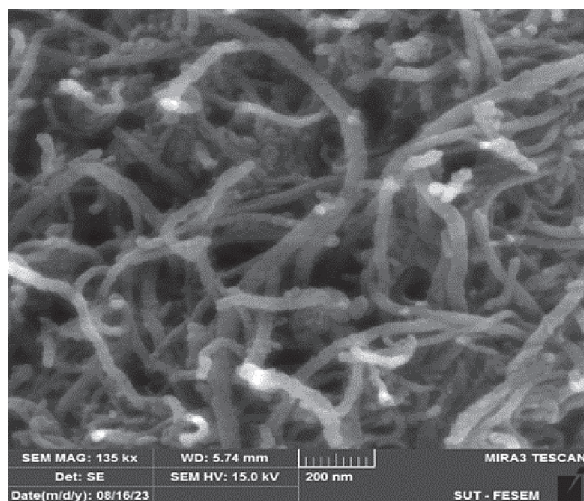


Figure 2. XRD patterns of raw MWCNTs

a)



b)

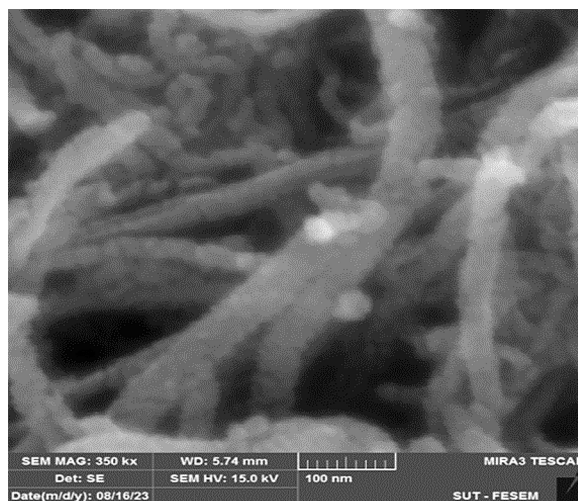


Figure 3. SEM image of MWCNTs (a) 135 \times magnification, (b) 350 \times magnification

a broad peak at 3348.42 cm^{-1} indicating O-H stretching vibrations. N-H stretching vibrations commonly found in primary or secondary amines are observed at 3248.13 cm^{-1} . The peak at 3086.11 cm^{-1} agrees to the C-H stretching vibrations in alkanes or aromatic compounds. The C-H stretching vibrations in alkenes or alkynes are specified by the peak at 2978.09 cm^{-1} . Peaks at 2881.65 cm^{-1} and 2823.79 cm^{-1} represent the C-H stretching vibrations in alkanes. A peak at 1712.79 cm^{-1} signifies the C=O stretching vibrations in carbonyl compounds such as ketones or aldehydes. At 1643.35 cm^{-1} , there are the C=C stretching vibrations in alkenes or aromatic compounds. The

peak at 1597.06 cm^{-1} agrees to the C=C stretching vibrations in aromatic compounds. The peak at 1523.76 cm^{-1} suggests the N-H bending vibrations in primary or secondary amines. Another peak at 1489.05 cm^{-1} indicates the C=C stretching vibrations in aromatic compounds. The peaks at 1450.47 cm^{-1} and 1400.32 cm^{-1} represent the C-H bending vibrations in alkanes. The C-N stretching vibrations in amines or amides are indicated by the peaks at 1330.88 cm^{-1} , 1249.87 cm^{-1} , and 1199.72 cm^{-1} . The peak at 1165.00 cm^{-1} agrees to the C-O stretching vibrations in esters or carboxylic acids. At 1114.86 cm^{-1} , there are the C-O stretching vibrations in alcohols or ethers. The

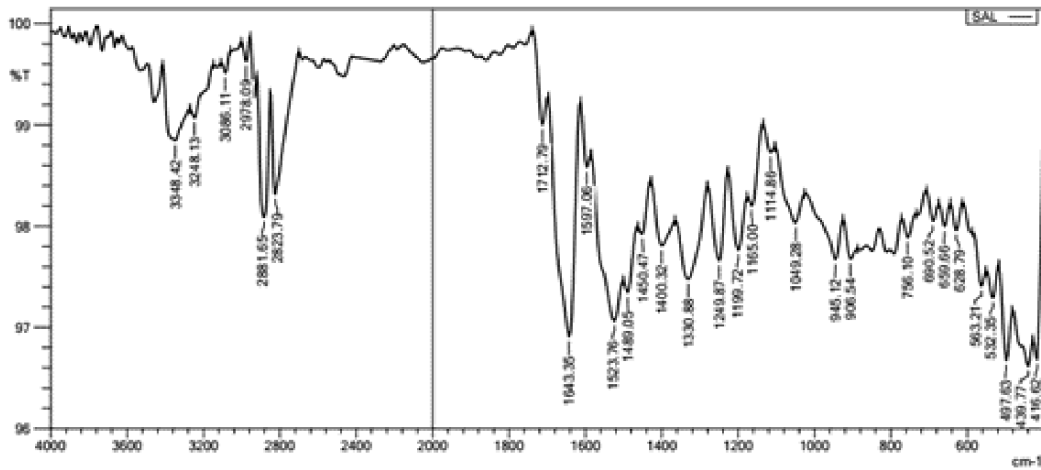


Figure 4. FTIR spectra of MWCNTs

peak at 1049.28 cm^{-1} signifies the C-O stretching vibrations in ethers or esters. The peaks at 945.12 cm^{-1} , 906.54 cm^{-1} , 756.10 cm^{-1} , and 690.52 cm^{-1} suggest the C-H bending vibrations in aromatic compounds. The peaks at 659.66 cm^{-1} , 628.79 cm^{-1} , 563.21 cm^{-1} , 532.35 cm^{-1} , 497.63 cm^{-1} , and 439.77 cm^{-1} correspond to the C-Cl stretching vibrations in alkyl chlorides. Lastly, the peak at 416.62 cm^{-1} indicates the C-H bending vibrations in aromatic compounds. It is important to note that interpreting FTIR spectra requires expertise, and considering the specific sample and its context is crucial. Accurate identification and characterization of functional groups or compounds often require further analysis and comparison with reference spectra (Salam et al. 2011; Sharmeen et al. 2018). Fig. 5 presents the results of a Zeta Potential analysis conducted

on (MWCNTs) using the SZ-100 instrument. The analysis gives information about the Zeta Potential and Electrophoretic Mobility of the sample. The measurement was performed at a temperature of 24.9°C using a dispersion medium at a viscosity of $0.897\text{ mPa}\cdot\text{s}$ and a conductivity of 0.208 mS/cm . The applied electrode voltage was 3.4 V . The results show three peaks in the Zeta Potential measurements, along with the corresponding values for Electrophoretic Mobility. The average Zeta Potential was determined to be -9.2 mV , while the average Electrophoretic Mobility was calculated as $-0.000071\text{ cm}^2/\text{Vs}$. The accompanying graph represents the distribution of Zeta Potential measurements for (MWCNTs), displaying a range of -400 to 500 mV on the x-axis and normalized intensity on the y-axis (Rehman et al. 2019).

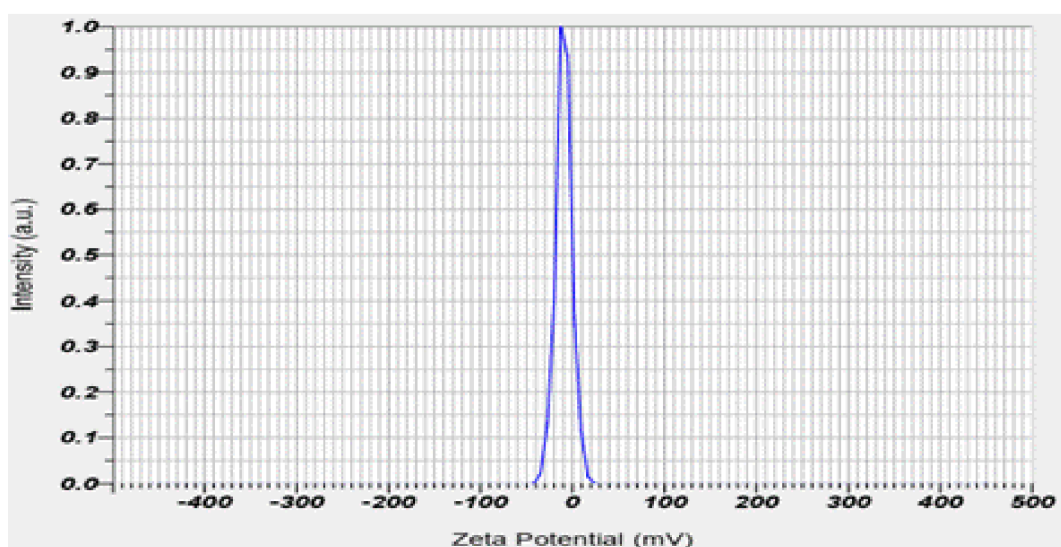


Figure 5. Zeta potential graphs of the MWCNTs

Variables affecting adsorption of dyes by MWCNTs

Effect of pH

Figure 6 depicts the effects of solution pH on methylene blue dye removal percentage by MCNTs. The pH value affects the dye adsorption process by modifying the surface charge of an adsorbent and the ionization behavior of the adsorbent and dye. It can be noticed that the methylene blue dye removal efficiency increases with rising pH from 2 to 8. The highest removal was reached at pH 6, with no increased adsorption at pH levels higher than 6. The existence of anionic groups on the surface of MWCNTs enhances their adsorption capacity through ion exchange and electrostatic interactions. The pH of the solution affects the competition between hydrogen ions and dye cations for sites of adsorption, with higher pH levels promoting better adsorption of cationic dyes onto MWCNTs (Moussavi and Khosravi 2010). Fig. 6 shows that with an increase in pH from 2 to 6, the removal percentage of Methylene Blue dye increased from 55%, 33%, 29%, and 20% to 98%, 97%, 92%, and 76% for initial dye concentrations of 20, 40, 90, and 100 mgL⁻¹, respectively, which is consistent with the findings reported by Mahvi et al. 2012 and Ibrahim et al. 2023.

Contact time effect

Figure 7. Illustrates the impact of contact time on the adsorption percentage of MB dye. Under these conditions, it was found that contact time of 60 min is enough to reach Methylene Blue dye equilibrium state. The results also determined that the adsorption process occurs rapidly at the beginning and then gradually approaches equilibrium. This phenomenon can be determined by the fact that during the initial stage, many free surface sites are available for sorption, while the staying free surface sites become increasingly difficult to occupy due to repulsive interactions between the phases (Garg et al. 2003), suggesting that the MWCNTs adsorption mechanism significantly varies depending on the structure of porous, requiring more time to diffuse through pores (Shrivastava and Wu, 2008). On the other hand, the adsorption sites on the cylindrical external wall of MWCNTs are typically found by the surface area and are unaffected by the inner wall spacing or inner cavities. These conclusions agree with those concluded by Mahvi et al. 2012 and Ibrahim et al. 2023.

Effect of MCNTs dosage

Figure 8 depicts the impact of MWCNT dosage on the Methylene Blue dye adsorption. Six doses of adsorbent were studied, i.e., 25, 40, 60, 70, 80, and 120 mg, to identify the optimal dosage of MWCNTs. The studied Methylene Blue dye concentrations were 20, 40, 70, and 120 mgL⁻¹. The pH of the solution was 6, and contact time was 60 min. Fig. 5 shows that, for 25 mg of MCNTs dosages, the found adsorption percentages were 62%, 55%, 45%, and 25% for the concentrations above, respectively. The adsorption percentages increased to 98%, 97%, 92%, and 75%, respectively, with increasing the MCNTs dosage to 100 mg. The adsorption rates increase because the larger surface area and the additional adsorption site profitable caused by more adsorbent doses, as reported by Mahvi et al. 2012 and Ibrahim et al. 2023. In addition, lower dosages

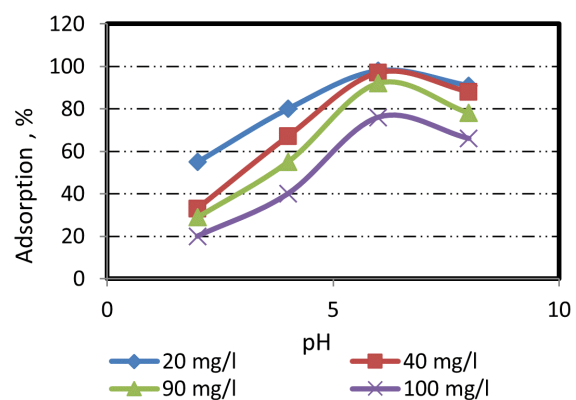


Figure 6. The pH impact on Methylene Blue dye adsorbed % in different initial dye concentrations (MCNTs dosage = 100 mg, contact time = 60 min)

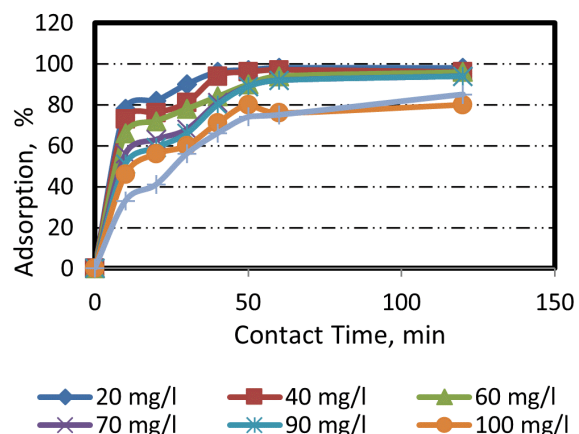


Figure 7. Contact time impact on Methylene Blue dye adsorbed % in different initial dye concentrations (pH = 6, MCNTs dosage = 100 mg)

result in more adsorption sites on the surface of MWCNTs for the target substances to combine with. However, increasing the dosage limits or saturates the number of available active sites. In other words, adding more MWCNTs creates no additional sites for the target substances to adsorb onto, causing diminishing returns regarding adsorption efficiency.

Effect of initial dye concentration

In Figure 9, the impact of initial dye concentration on the Methylene Blue dye removal using MWCNTs was explained. The Methylene Blue dye percentage removal increases as the initial dye concentration decreases. The highest removal was investigated at a dye concentration of 20 mgL⁻¹. The highest removal percentage was 78% as the initial concentration was 120 mgL⁻¹. However, reducing the concentration to 20 mgL⁻¹ increases the removal percentage to 98%. The observed trend was caused by the unoccupied surface sites abundance on the MWCNTs useful for molecules of dye adsorption. The low dye initial concentration is accompanied by more vacant surface sites, increasing the dye adsorption percentage. However, as the concentration initial dye rises, the remaining surface site occupation becomes more challenging because the repulsion between the dye molecules on the MWCNTs. Consequently, the percentage of dye removal decreases. The maximum removal percentage is an important factor that indicates the efficiency of MWCNTs as an adsorbent material for the colorization of MB dye. The findings can be used to optimize the operating conditions, like initial dye concentration, to achieve the highest removal efficiency (Mahvi et al. 2012). Increasing dye concentrations in real applications, can increase adsorbent dosage, enhance adsorbent properties through various methods, like functionalization or surface modification of the adsorbent, which can increase its surface area, introduce specific functional groups, or and enhance its affinity for the target dyes. By improving the adsorption characteristics of the adsorbent, its effectiveness in removing higher concentrations of dyes can be enhanced.

Equilibrium isotherm models

Equilibrium Adsorption refers to the state at which the adsorption process reaches a balance between the adsorbent (material on which

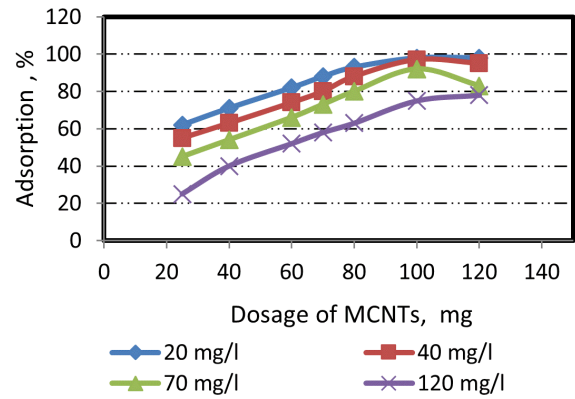


Figure 8. MCNT Dosage impact on Methylene Blue dye adsorbed % in different initial dye concentrations (pH = 6, Time = 60 min)

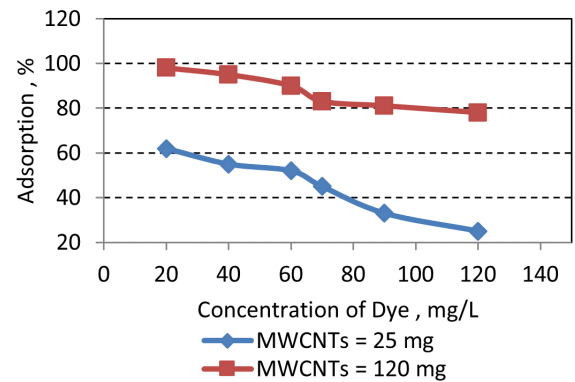


Figure 9. Initial MB dye concentration effect on adsorbed % in different dosages of MCNTs (pH = 6, contact time = 60 min)

adsorption occurs) and the adsorbate (substance being adsorbed). At equilibrium, desorption rate is equal to adsorption rate, resulting in a stable adsorbate concentration on the surface of the adsorbent. In the context of adsorption, equilibrium is typically described by an adsorption isotherm, which represents the relationship between the quantity of adsorbate adsorbed onto the adsorbent at equilibrium and the concentration of the adsorbate in the surrounding solution. The present study assessed the ability of equilibrium isotherm models, Langmuir, Freundlich, and Temkin to explain the adsorption equilibrium properties. The quantity of Methylene Blue dye adsorbed on the MWCNTs surface at equilibrium state and the dye residual concentration in solution relationship is defined by an adsorption isotherm, representing the solute, i.e., Methylene Blue dye, equilibrium adsorption behavior onto an adsorbent, i.e., MWCNTs, describes the solute distribution between the aqueous phase and adsorbent surface at a

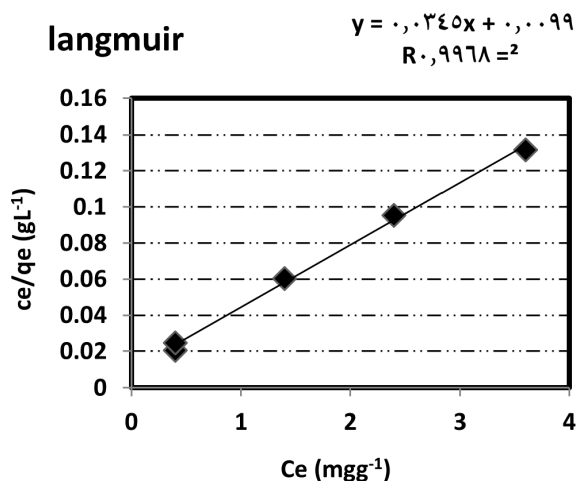


Figure 10. Langmuir isotherm model for MB dye; initial concentration = 20 mgL⁻¹, pH = 6, MWCNT dosage = 100 mg, time = 60 min, and solution volume = 100 ml

certain temperature. Fig. 10 shows the Langmuir isotherm plot (C_e/q_e vs. C_e) for the experimental results. A high correlation can be seen between the Langmuir model and experimental results. The Langmuir isotherm model produced an R^2 of 0.9968, showing a solid correspondence between the experimental and theoretical results. The Langmuir isotherm model is founded on various assumptions: (i) the adsorption happens at discrete locations on the adsorbent material surface, (ii) each location can solely accommodate one adsorbate molecule, (iii) there is no relation between the adsorbed molecules, and (iv) the adsorption process is double. On the basis of these assumptions, the Langmuir isotherm equation can be employed to find the highest adsorption capacity and the adsorption process equilibrium constant of the adsorbent material.

The good agreement between experimental data and the Langmuir isotherm model, as evidenced by the high R^2 value obtained, indicates that the Methylene Blue dye adsorption onto MWCNTs follows a monolayer adsorption mechanism. This finding has important implications, as it suggests the Langmuir isotherm model can be applied to predict the equilibrium adsorption capacity of MWCNTs for Methylene Blue dye with a high degree of accuracy. The equilibrium parameter R_L , which has no dimensions, is the same as $(1/(1+K_f C_e))$. Table 1 demonstrates that activated carbon favors MB adsorption (Peng and Luan, 2003).

Figure 11 presents the Freundlich isotherm models plot for the adsorption data of MB dye

by MWCNTs. The figure shows the relationship between $\log q_e$ and $\log C_e$. The R^2 value obtained from the Freundlich isotherm model was 0.8999, designating a moderate fit of the data experimental to the theoretical model.

Figure 12 displays the Temkin isotherm model plot for the adsorption data of MB dye by MWCNTs. The plot shows the relationship between the natural logarithm of the concentration of Methylene Blue dye in the solution (C_e) and the quantity of dye adsorbed on the surface of MWCNTs at equilibrium (q_e). The R^2 obtained from the Temkin isotherm model was 0.9292, indicating a suitable fit of the experimental data to the theoretical model. Table 1 provides additional information on the isotherm models explained

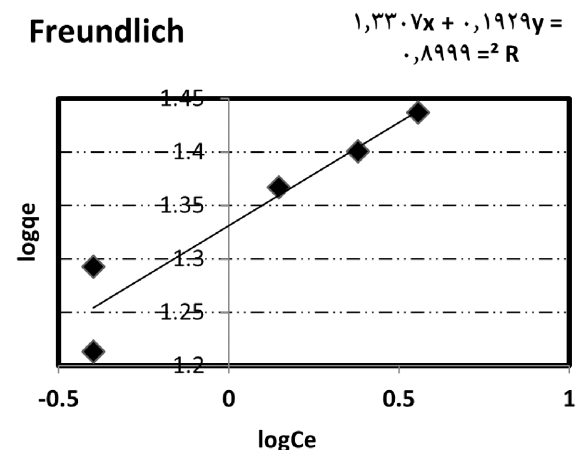


Figure 11. Freundlich isotherm model for MB dye; initial concentration = 20 mgL⁻¹, pH = 6, MWCNT dosage = 100 mg, time = 60 min, and solution volume = 100 ml

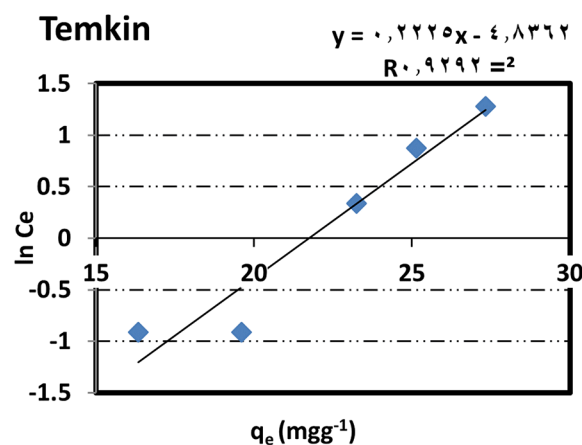


Figure 12. Temkin isotherm model for Methylene Blue dye; initial concentration = 20 mgL⁻¹, pH = 6, MWCNT dosage = 100 mg, time=60 min, and solution volume = 100 ml

Table 1. Isotherms models details of methylene adsorption by MWCNTs

Isotherms Model	Parameters	value	R ²
Langmuir	q _m (m _g g ⁻¹)	28.98	0.9968
	K _c (Lm _g ⁻¹)	3.48	
	R _l	0.01414	
Freundlich	1/n	5.184	0.8999
	K _f (m _g g ⁻¹)	21.414	
Temkin	B ₁	0.2225	0.9292
	LnK ₁	21.735	

in this study, including the parameters and equations explained to fit the experimental data. The results show that the Langmuir isotherm model with R²=0.9968 provided the good fit with data experimental of adsorption. Table 2 presents some of the highest adsorption capacities of different adsorbents for different dyes under different experimental conditions documented in the literature. Table 2 shows that MWCNTs are more efficient than other adsorbents in removing dyes from aqueous solutions. However, it is not possible to make a direct comparison of the various adsorbents due to the variability of experimental conditions used in different studies.

Kinetic models

The three most well-known models of kinetic, pseudo-first-order, pseudo-second order, and Weber–Morris, were utilized in this investigation to describe the method by which Methylene Blue adsorbs onto MWCNTs. The experimental data were collected with the initial concentration

of 20 mgL⁻¹, MWCNT dosage of 100 mg, equilibrium time of 60 minutes, and pH 6. Figure 13 through 15 show the plot models of kinetic. In pseudo-second order, it is evident that a higher R² has been achieved. Regarding the R² value of pseudo-second order (0.9982), it is evident that

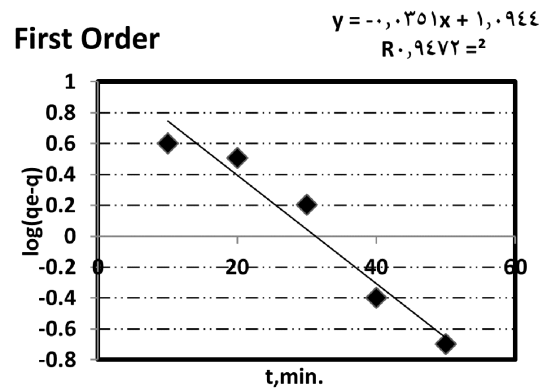


Figure 13. Model of pseudo-first order kinetics; pH = 6, initial dye concentration = 20 mgL⁻¹, MWCNT dosage = 100 mg, time = 60 min, and solution volume = 100 ml.

Table 2. Some of the adsorption capacities (q_e) of different adsorbents for different types of dyes

Adsorbent	Adsorbate	Condition	Capacity for adsorption, m _g g ⁻¹	Ref.
MWCNTs	Methylene Blue	pH = 6 Con = 20 mgL ⁻¹ , Dose = 100 mg T = 25°C	19.6	Present work
MWCNTs	Acid Red 18	pH = 5, Con. = 25mgL ⁻¹ , Dose = 0.2 gL ⁻¹ , T = 25°C	166.67	[2]
MWCNTs- Fe ₂ O ₃	Methylene Blue Neutral Red	pH = 6.0 Co = 20 mgL ⁻¹ , Dose = 0.1 gL ⁻¹ T = 25°C	42.3 77.5	[41]
MWCNTs	Methylene Blue	pH = 6 Con. = 10 mgL ⁻¹ Dose = 0.4 gL ⁻¹ T = 17°C	103.62	[42]
Activated carbon. Activated carbon from Cordi Myxa	Methylene Blue Methylene Blue	Con. = 150 mgL ⁻¹ T = 25°C	40.06	[43]
		Con. = 30 mgL ⁻¹ Dose = 2 gL ⁻¹	71.43	[44]

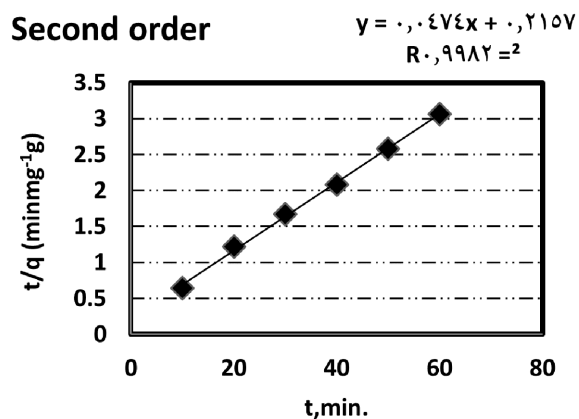


Figure 14. Model of pseudo-second order kinetics; pH = 6, initial dye concentration = 20 mgL⁻¹, MWCNT dosage = 100 mg, time = 60 min, and solution volume = 100 ml

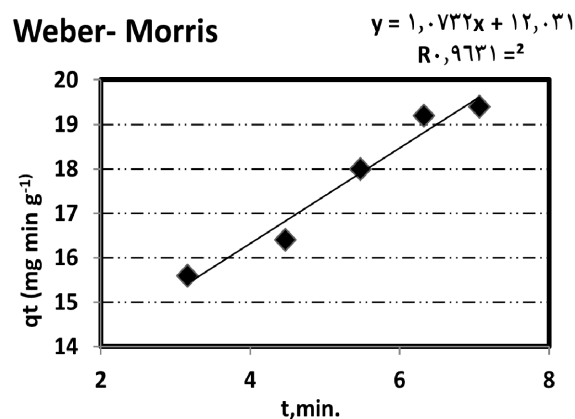


Figure 15. Kinetic model of Weber–Morris; pH = 6, initial dye concentration = 20 mgL⁻¹, MWCNT dosage = 100 mg, time = 60 min, and solution volume = 100 ml

Table 3. Adsorption kinetics of methylene blue multiwall carbon nano tubes

Kinetic models	Parameters	Pseudo first order	Pseudo second order	Weber–Morris
Initial concentration 20 mgL ⁻¹	R ²	0.9472	0.9982	0.9631
	Constant	K ₁ = 0.0808	K ₂ =0.0104	K _{id} = 1.073
	q _e	12.47	21.1	-----

this is the model’s best fit conformity. As a result, the dye’s adsorption mechanism on the surface of MWCNT appears to be consistent with the second-order model. Table 3 summarizes the correlation coefficients and the kinetics of Methylene Blue adsorption.

CONCLUSIONS

Dyes are used broadly in numerous industries; however, they significantly threaten humans and aquatic life. Consequently, it is vital to treat the wastewater that contains dyes before its release. Adsorption is a common technique because of various advantages, i.e., simplicity and accessibility. The present study demonstrates MWCNTs as an effective adsorbent to remove the dye. The present study revealed that the highest MB dye adsorption removal on MWCNTs was 98% at pH = 6, 20 mgL⁻¹ initial concentration, 100 mg MWCNT dosage, and at 25°C. The Langmuir isotherm (R² = 0.9968) and the pseudo-second-order model (R² = 0.9982) well-described the Methylene Blue dye by MWCNTs adsorption results. As a result, MWCNTs can be shown as a promising potential as adsorbents for Methylene Blue dye colorization from aqueous solutions.

The present findings recommend MWCNTs as a highly effective, reliable adsorbent material, environmentally friendly, and low-cost solution to treat aqueous solutions-containing dyes. Thus, due to their durability and superior adsorption performance, MWCNTs are a promising technique for the wastewater treatment industry.

Acknowledgment

The authors thank the central laboratories of Tikrit University, Iraq, for their support in conducting the laboratory examinations.

REFERENCES

- Robati D., Mirzab B., Ghazisaeidic R., Rajabid M., Moradie O., Tyagif I., Shilpi A. G., and Gupta V. K. 2016. Adsorption behavior of methylene blue dye on nanocomposite multi-walled carbon nanotube functionalized thiol (MWCNT-SH) as a new adsorbent. *Journal of Molecular Liquids*. 216, 1: 830–835.
- Shirmardi M., Mesdaghinia A., Mahvi A. H., Nasseri S., and Nabizadeh R. 2012. Kinetics and equilibrium studies on adsorption of acid red 18 (Azo-Dye) using multiwall carbon nanotubes (MWCNTs) from aqueous solution. *E-Journal of Chemistry*. 9, 4: 2371–2383.

3. Almhana N. M., Naser Z. A., Al-Najjar S. Z., Al-Sharif Z. T., and Nail T. H. 2022. Photocatalytic Degradation of Textile Dye from Wastewater by using ZnS/TiO₂ Nanocomposites Material. *Egyptian Journal of Chemistry*, 65,13: 481 – 488. <https://dx.doi.org/10.21608/ejchem.2022.125852.5588>.
4. Sanghavi B. J., Varhue W., Rohani A., Liao K., Bazydlo L.A.L., Chou C.-Fu, and Swami N.S. 2015. Ultrafast immunoassays by coupling dielectrophoretic biomarker enrichment in nanoslit channel with electrochemical detection on graphene. *Lab on a Chip*, 15, 24: 4563–4570.
5. Ghosh S., Falyouna O., Malloum A., Othmani A., Bornman C., Bedair H., Onyeaka H., Al-Sharif Z. T., Jacob A. O., Miri T., Osagie C., and Ahmadi Sh. 2022a. A general review of the use of advanced oxidation and adsorption processes for the removal of furfural from industrial effluents. *Microporous and Mesoporous Materials*, 331, 2022: 1387-1811.
6. Altıntig E., Altundag H., Tuzen M., and Sari A. 2017. Effective removal of methylene blue from aqueous solutions using magnetic loaded activated carbon as novel adsorbent. *Chemical Engineering Research and Design*, 122: 151-163.
7. Ibrahim A.K. 2021. Improvement of removal efficiency of water supply plant by using polyelectrolyte type LT-22 with alum. *Material Today Process*, 42:1928-1933.
8. Ahmed S.H., Al-Jubouri S.M., Zouli N. Ahmed A. Mohammed A.A., Majdi H.S., Salih I. K., Al-shaeli M., Al-Rahawi A.M.I., Alsahy Q.F., and Alberto Figoli A. 2021. Performance Evaluation of Polyethersulfone Membranes for Competitive Removal of Cd²⁺, Co²⁺, and Pb²⁺ Ions from Simulated Groundwater. *Geofluids*, 2021, 1:11. <https://doi.org/10.1155/2021/6654477>
9. Ghosh S., Othmani A., Malloum A., Christ Ke. O., Onyeaka H., AlKafaas S.S., Nnaji N.D., Bornman C., Al-Sharif Z.T., Ahmadi S., Dehghani M.H., Mubarak N.M., Tyagi I., Karri R.R., Koduru J.R., 2022b. Removal of mercury from industrial effluents by adsorption and advanced oxidation processes: A comprehensive review. *Journal of Molecular Liquids*, 367: 120491.
10. Mohammed H. A., Khaleefa S. A., and I. Basheer M.I. 2021. Photolysis of Methylene Blue Dye using an Advanced Oxidation Process (Ultraviolet Light and Hydrogen Peroxide). *Journal of Engineering and Sustainable Development*, 25, 1: 59–67. <https://doi.org/10.31272/jeasd.25.1.5>
11. Badran I., and Khalaf R. 2020. Adsorptive removal of alizarin dye from wastewater using maghemite nano adsorbents. *Separation of Science and Technology*, 55,14: 2433–2448. <https://doi.org/10.1080/01496395.2019.1634731>
12. Li Y., Du. Q., Li. T., Sun J., Wan Y., Wu S., Wang Z., Xia Y., and Xia L. 2013. Methylene blue adsorption on graphene oxide/calcium alginate composites. *Carbohydrate Polymers*, 95, 1, 501-507.
13. Machado F.M., Bergmann C.P., Fernandes T.H.M., Lima E.C., Royer B., Calveteb T., and Faganc S.B. 2011. Adsorption of reactive red M-2BE dye from water solutions by multi-walled carbon nanotubes and activated carbon. *Journal of Hazard Materials*, 192:1122–1131.
14. Fan L., Luo C., Sun M., Qiu H., and Li X. 2013. Synthesis of magnetic β -cyclodextrin chitosan/graphene oxide as nano adsorbent and its application in dye adsorption and removal. *Colloids and Surfaces B: Biointerfaces*, 103, 1: 601-607.
15. Georgiou D., Petrolekas P. D., Hatzixanthis S., and Aivasidis A. 2007. Adsorption of carbon dioxide by raw and treated dye-bath effluents. *Journal of Hazardous Materials*, 144, 1-2: 369-376.
16. Saleh T.A., and Gupta V.K. 2012. Photo-catalyzed degradation of hazardous dye methyl orange by use of a composite catalyst consisting of multi-walled carbon nanotubes and titanium dioxide. *Journal of Colloid and Interface Science*, 371, 1,101-106.
17. Onal Y. 2006. Kinetics of adsorption of dyes from aqueous solution using activated carbon prepared from waste apricot. *Journal of Hazardous Materials*, 137, 3: 1719-1728.
18. Ahmed S.H. 2017. Cu II Removal from Industrial Wastewater Using Low-Cost Adsorbent. *Tikrit Journal of Engineering Sciences*, 24, 2: 44-50.
19. Mohammed M.I., Abdul Razak A.A., and Al-Timimi D.A.H. 2014. Modified Multi-walled Carbon Nanotubes for Treatment of Some Organic Dyes in Wastewater. *Advances in Materials Science and Engineering*, 2014,10. <http://dx.doi.org/10.1155/2014/201052>
20. Mohsen E.N., Hussien T.K., and Jasim A.N. 2023. Cd²⁺ Sorption from Aqueous Solution using Rosemary Plant: Performance and Isotherm Study. *Journal of Engineering and Sustainable Development*, 27, 3: 407–416. <https://doi.org/10.31272/jeasd.27.3.10>
21. Muhaisen L.F., Al-Najjar S.Z., and Al-Sharif Z.T. 2020. Modified orange peel as a sorbent in removing heavy metals from aqueous solution. *Journal of Green Engineering*, 10, 11: 10600-10615.
22. Sahu S., Pahi S., Sahu J.K., Sahu U.K., and Patel R.K. 2020. Kendu (*Diospyros melanoxylon* Roxb) fruit peel activated carbon—an efficient bio adsorbent for methylene blue dye: Equilibrium, kinetic, and thermodynamic study. *Environmental Science Pollution Research*, 27: 22579–22592.
23. Sabar S., Abdul Aziz H., Yusof N.H., Subramaniam S., Foo K.Y., Wilson L.D., and Lee H.K. 2020. Preparation of sulfonated chitosan for enhanced adsorption of methylene blue from aqueous solution. *Reactive*

- and Functional Polymers. 151:104584.
24. Moussavi G.R., and Khosravi R. 2010. Removal of cyanide from wastewater by adsorption onto pistachio hull wastes: Parametric experiments, kinetics, and equilibrium analysis. *Journal of Hazardous Materials*.183, 1-3: 724-730.
 25. Hong S., Wen C., He J., Gan F., and Ho Y. S. 2009. Adsorption thermodynamics of Methylene Blue onto bentonite. *Journal of Hazardous Materials*.167,1-3: 630-633.
 26. Baccar R., Bouzid J., Feki M., and Montiel A. 2009. Preparation of activated carbon from Tunisian olive-waste cakes and its application for adsorption of heavy metal ions. *Journal of Hazardous Materials*. 162, 2-3:1522-1529.
 27. Ahmed S.H., Ibrahim A.K., Abed M.F. 2023. Assessing the quality of groundwater and the nitrate exposure, North Salah Al-Din Governorate. *Iraq. Tikrit Journal of Engineering Sciences*.30, 1: 25-36.
 28. Weber T.W., and Chakkravorti R.K. 1974. Pore and solid diffusion models for fixed bed adsorbers. *AIChE Journal* 20: 228-232.
 29. Chen C., Hu J., Shao D., Li J., Wang X. 2009. Adsorption behavior of multiwall carbon nanotube/iron oxide magnetic composites for Ni (II) and Sr (II). *Journal of hazardous materials*. 164: 923-928.
 30. Gupta V. K., Agarwal S., and Saleh T.A. 2011. Synthesis and characterization of alumina-coated carbon nanotubes and their application for lead removal. *Journal of hazardous materials*.185: 17-23.
 31. Oh W.-C., Zhang F.-J., and Chen M.-L. 2010. Characterization and photodegradation characteristics of organic dye for Pt–titania combined multi-walled carbon nanotube composite catalysts. *Journal of industrial and engineering chemistry*. 16: 321-326.
 32. Jurkiewicz K., Pawlyta M., and Burian A. 2018. Structure of carbon materials explored by local transmission electron microscopy and global powder diffraction probes. *C, MDPI*. 4, 68.
 33. Abdel-Ghani N.T., El-Chaghaby G.A., and Helal F.S. 2015. Individual and competitive adsorption of phenol and nickel onto multiwalled carbon nanotubes. *Journal of advanced research*. 6: 405-415.
 34. Robati D., Mirza B., Ghazisaeidi R., Rajabi M., Moradi O., Tyagi I., Agarwal S., and Gupta V.K., 2016. Adsorption behavior of methylene blue dye on nanocomposite multi-walled carbon nanotube functionalized thiol (MWCNT-SH) as new adsorbent. *Journal of Molecular Liquids*. 216: 830-835.
 35. Salam M.A., Makki M.S.I., and Abdelaal M.Y.A. 2011. Preparation and characterization of multi-walled carbon nanotubes/chitosan nanocomposite and its application for the removal of heavy metals from aqueous solution. *Journal of Alloys and Compounds*. 509: 2582-2587.
 36. Sharmeen S., Rahman A.F.M.M., Lubna M.M., Salem K.S., Islam R., Khan M.A. 2018. Polyethylene glycol functionalized carbon nanotubes/gelatin-chitosan nanocomposite: An approach for significant drug release. *Bioactive materials*. 3: 236-244.
 37. Rehman W.U., Merican Z.M.A., Bhat A.H., Hoe B.G., Sulaimon A.A., Akbarzadeh O., Khan M.S., Mukhtar, A., Saqib, S., and Hameed, A. 2019. Synthesis, characterization, stability, and thermal conductivity of multi-walled carbon nanotubes (MWCNTs) and eco-friendly jatropa seed oil based nanofluid: An experimental investigation and modeling approach. *Journal of Molecular Liquids*. 293: 111534.
 38. Garg V.K., Gupta R., Yadav A.B., and Kumar R. 2003. Dye removal from aqueous solution by adsorption on treated sawdust. *Bioresource Technology*. 89, 2: 121-124.
 39. Shrivastava K., and Wu H.-F. 2008. Functionalized-multiwalled carbon nanotubes as a pre-concentrating probe for rapid monitoring of cationic dyes in environmental water using APMALDI/MS. *Journal of Separation Science*. 31, 20: 3603-3611.
 40. Peng X., Li Y., and Luan Z. 2003. Adsorption of 1,2-dichlorobenzene from water to carbon nanotubes. *Chemical Physics Letters*. 376, 1-2: 154-158. DOI:
 41. Qu S., Huang F., Yu h., Chenc G., and Kong J. 2008. Magnetic removal of dyes from aqueous solution using multi-walled carbon nanotubes filled with Fe₃O₄ particles. *Journal of Hazardous Materials*. 160, 2-3: 643-647. DOI:
 42. Shahryari Z., Goharrizi AS., and Azadi M. 2010. Experimental study of methylene blue adsorption from aqueous solutions onto carbon nano tubes. *International Journal of Water Research and Environmental Engineering*. 2: 16-28.
 43. Sharma Y.C., Upadhyay S.N., and Gode F. 2009. Adsorptive removal of a basic dye from water and wastewater by activated carbon. *Journal of Applied Science Environmental Sanitation*. 4, 1: 21-28.
 44. Ibrahim . K., Ahmed, S.H., & Abduljabbar, R.A. 2023. Removal of methylene blue dye from aqueous solutions using cordia myxa fruits as a low-cost adsorbent. *Tikrit Journal of Engineering Sciences*. 30, 3: 90–99. <https://doi.org/10.25130/tjes.30.3.10>